Band-Gap and Band-Edge Engineering of Multicomponent Garnet Scintillators from First Principles

Satyesh K. Yadav, Blas P. Uberuaga, Martin Nikl, Chao Jiang, and Christopher R. Stanek

Phys. Rev. Applied **4**, 054012 — Published 24 November 2015

DOI: 10.1103/PhysRevApplied.4.054012

Band-gap and Band-edge Engineering of Multicomponent Garnet Scintillators: A First-principles Study

Satyesh K. Yadav* and Blas P. Uberuaga
Materials Science and Technology Division, Los Alamos National Laboratory, Los Alamos, NM 87545, USA

Martin Nikl
Institute of Physics, Academy of Sciences of the Czech Republic, 16253 Prague, Czech Republic

Chao Jiang
Thermo-Calc Software Inc., Pittsburgh, PA 15317, USA

Christopher R. Stanek
Materials Science and Technology Division, Los Alamos National Laboratory, Los Alamos, NM 87545,USA

Complex doping schemes in $RE_3Al_5O_{12}$ (RE=rare earth element) garnet compounds have recently led to pronounced improvements in scintillator performance. Specifically, by admixing lutetium and yttrium aluminate garnets with gallium and gadolinium, the band-gap was altered in a manner that facilitated the removal of deleterious electron trapping associated with cation antisite defects. Here, we expand upon this initial work to systematically investigate the effect of substitutional admixing on the energy levels of band-edges. Density functional theory (DFT) and hybrid density functional theory (HDFT) was used to survey potential admixing candidates that modify either the conduction band minimum (CBM) or valence band maximum (VBM). We considered two sets of compositions based on $Lu_3B_5O_{12}$ where B = Al, Ga, In, As, and Sb; and $RE_3Al_5O_{12}$, where RE = Lu, Gd, Dy, and Er. We found that admixing with various RE cations does not appreciably effect the band-gap or band-edges. In contrast, substituting Al with cations of dissimilar ionic radii has a profound impact on the band structure. We further show that certain dopants can be used to selectively modify only the CBM or the VBM. Specifically, Ga and In decrease the band-gap by lowering the CBM, while As and Sb decrease the band-gap by raising the VBM, the relative change in band-gap is quantitatively validated by HDFT. These results demonstrate a powerful approach to quickly screen the impact of dopants on the electronic structure of scintillator compounds, identifying those dopants which alter the band-edges in very specific ways to eliminate both electron and hole traps responsible for performance limitations. This approach should be broadly applicable for the optimization of electronic and optical performance for a wide range of compounds by tuning the VBM and CBM.

I. INTRODUCTION

$A_3B_5O_{12}$ garnets, and in particular $RE_3Al_5O_{12}$ compositions (where RE is rare earth element or Y), have been studied for technical use as optical materials for over 50 years [1–3]. Although garnets also received interest as a scintillator ∼20 years ago [4], a lower light yield than other compounds ultimately led to relative disinterest. Often, defects trap charge carriers, otherwise available to participate in the scintillation process, thus potentially resulting in delayed and/or reduced light output. The important role that defects play in scintillator performance has been well-documented [5]. However, recent studies involving co-doping of garnets have demonstrated dramatic improvements in light yield and these findings have consequently reinvigorated interest in garnets as high performance scintillators [6–16]. These optimization efforts have relied on the manipulation of the garnet electronic structure through admixing, and in the process creating so-called "multicomponent" garnets [17]. It is well-known that cation antisite defects are present in garnets (RE^{3+} on Al^{3+} sites and vice versa) [18–23] and that they contribute to reduced scintillator performance [24] by creating traps for the electronic carriers which results in considerable slowing down of scintillation response. However, the challenge of removing cation antisite defects in garnet is that they are isovalent (i.e. charge neutral) and the corresponding defect formation energy is rather low, thereby preventing a defect engineering approach. Therefore alternative defect management methods are required. Interestingly, it has been shown that adding Ga to aluminate garnets removes the signature of antisite defects [25]. This implies that Ga admixing eliminates the effectiveness of the antisite traps. However, Ga is closer in size to the RE cation than it is to Al [26], which suggests that a higher concentration of antisites should exist in Ga-doped garnets than in pure aluminate garnets - a hypothesis validated by a joint experimental-atomistic simulation study [27, 28]. Rather, instead of reducing the concentration of deleterious antisite defects, the benefit of Ga-admixing arises from shifts in the conduction band such that it envelops the trap state in the forbidden gap associated with the antisite defect [17, 29]. This is a primary example of the "band-gap engineering" approach to defect management.

* syadav@lanl.gov, yadav.satyesh@gmail.com

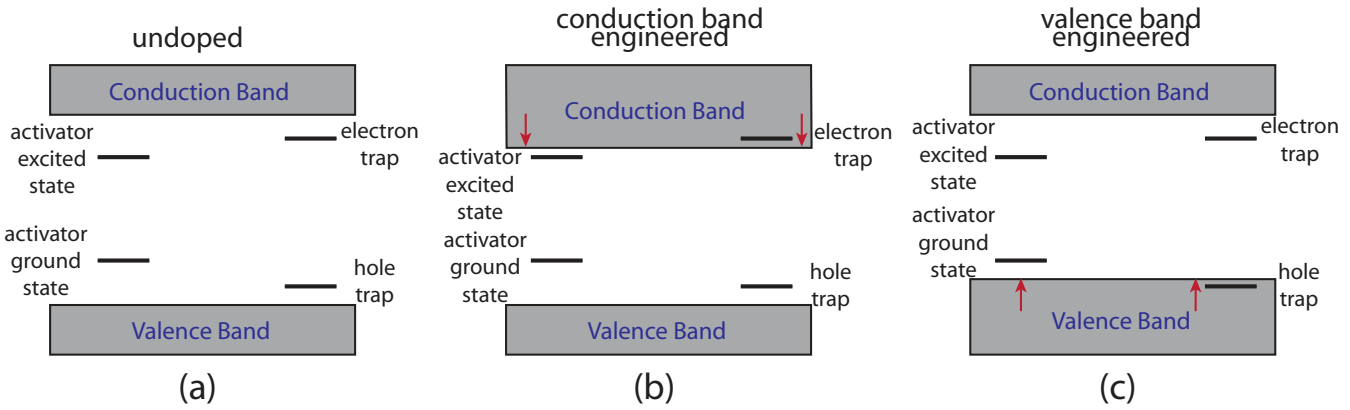

FIG. 1. A simplified schematic showing activator transition levels and electron and hole traps with respect to valence and conduction band-edges of a scintillator, where (a) is the case of an undoped scintillator, where both electron and hole traps reside within the band-gap, (b) illustrates the idealized scenario of the same scintillator that has been strategically doped to shift only the conduction band-edge in order to envelop the electron trap (but not the excited state of the activator) and (c) shows the analogue case for the scintillator doped to modify the valence band-edge in order to envelop the hole trap (but not the activator ground state). Specific shifting of band-edges is what is referred to as "band-edge engineering."

In this paper, we build upon our previous effort to optimize the electronic structure of multicomponent garnets by studying a range of dopants and their effect on the energy levels of band-edges of $Lu_3Al_5O_{12}$. Our approach relies on manipulation of the electronic structure of a scintillator compound through doping in order to remove the deleterious effect of defects that may act as electron or hole traps. A key aspect of this approach is that the band-edges must be shifted to envelop the shallow trap states, without also interfering with the activator transition. A simplified schematic showing the position of activator transition levels (with no splitting for illustration purposes) and electron and hole traps with respect to valence and conduction band is presented in Fig. 1. Band-edges can be modified by doping to shift valence and conduction band. The level of band-edges modified due to doping should only eliminate the defect states but should not lower the CBM or raise the VBM to an extent that Ce^{3+} transition levels fall in the conduction or valence bands. By using density functional theory (DFT) based first-principles calculations, we show that certain 3+ dopants that substitute for Al can result in variations in either the valence or conduction band-edges, while leaving the other band-edge more or less unchanged - thus opening the path for "band-edge engineering" through admixing. We also show that substituting Lu with RE cations does not have a significant impact on band-edges. Although we use garnet as a case study, it is anticipated that this approach can be extended to a wide range of scintillator compounds and provide an efficient manner to screen dopants for optimizing performance.

II. METHODOLOGY

A. First-principles method

Density functional theory (DFT) calculations were performed using the Vienna *Ab initio* Simulation Package (VASP) [30]. The DFT calculations employed the Perdew, Burke, and Ernzerhof (PBE) [31] generalized gradient approximation (GGA) exchange-correlation functional and the projector-augmented wave (PAW) method [32]. The hybrid DFT calculations utilized the specific functional referred to as the HSE06 functional in the literature[33]. This functional is created by starting with the PBE exchange-correlation functional and replacing 25% of the PBE exchange interaction by a screened nonlocal functional with an inverse screening length of $0.2Å^{-1}$. For all calculations, a plane wave cutoff of 500 eV for the plane wave expansion of the wave functions was used to obtain highly accurate forces. In the results reported, only the gamma point was considered in the k-space sampling; however, we have employed denser k-point meshes in select cases and very similar results were obtained. All structures were fully relaxed without any symmetry constraints and relaxations were considered converged when each component of the force on every atom was smaller than 0.02 eV/Å.

B. Band-edge alignment

The first step to reliably determine the relative position of band-edges in a compound as a function of composition is to identify a reference state that does not change with chemical composition. There are several references that are used in the literature to determine the relative position of band-edges [34–37]. The average electrostatic

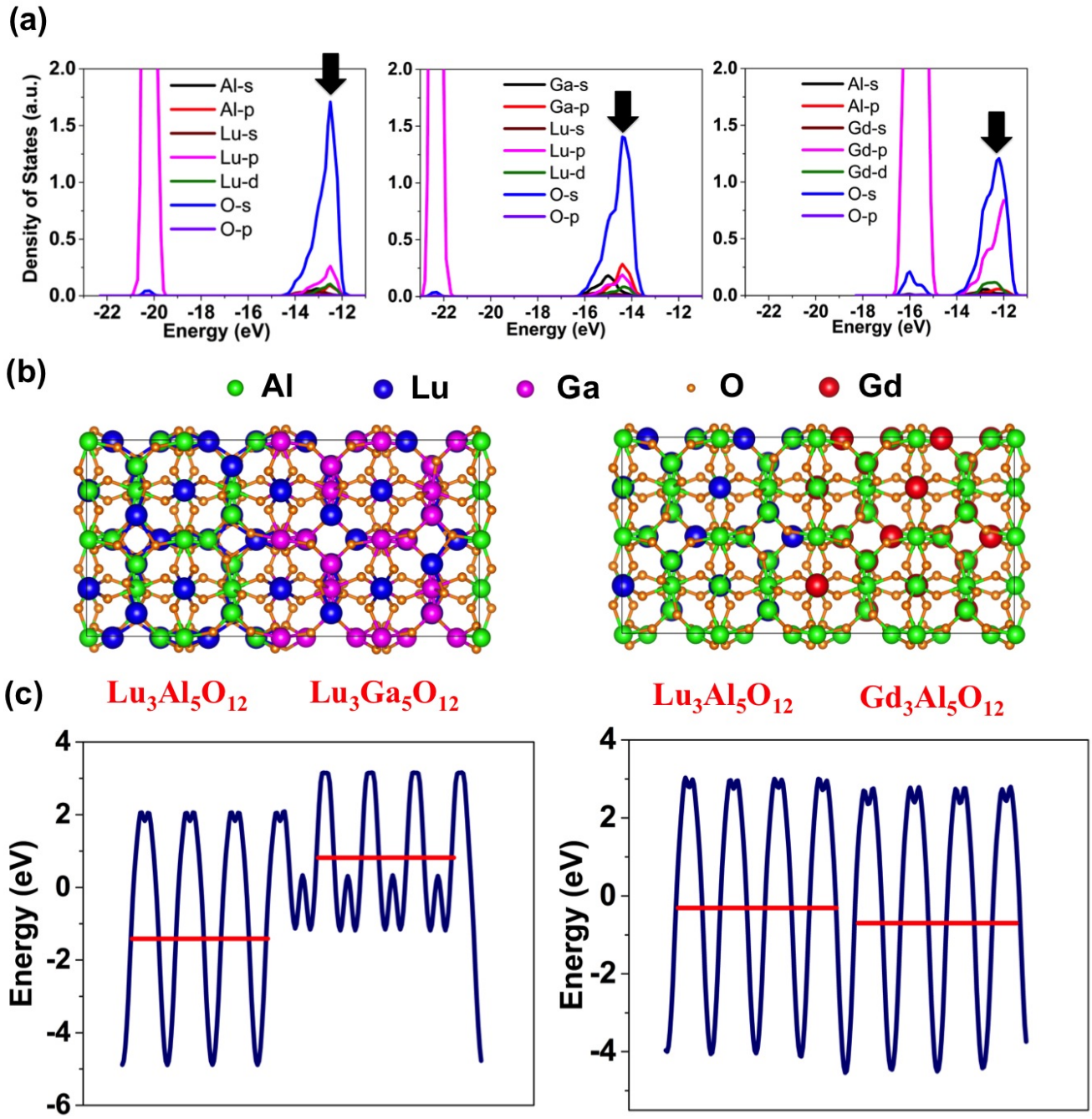

FIG. 2. (a) Density of states of deep states of $Lu_3Al_5O_{12}$, $Lu_3Ga_5O_{12}$, and $Gd_3Al_5O_{12}$, where the oxygen state that is used as a reference is marked by an arrow. (b) Supercell used for calculating electrostatic potentials, where Lu is blue, Al green, Ga magenta, O orange, Gd red. (c) Electrostatic potential calculated using the supercell in (b), where the red horizontal line indicates the average electrostatic potential.

potential is the best common reference but it is very expensive to calculate as both materials of interest must be contained within one common simulation cell. Not only does this necessitate large cells to accommodate both materials, but also to avoid interfacial effects that are not of interest here. Rather than rely on computationally intensive electrostatic potential approach, in this work we use a deep 2 s state of oxygen as a reference to realign band-edges of two compounds [34].

Figure 2(a) shows the density of states (DOS) plot of $Lu_3Al_5O_{12}$, $Lu_3Ga_5O_{12}$, and $Lu_3Gd_5O_{12}$, and the s state chosen for comparison is indicated by an arrow. It can be seen in Figure 2(a) that the deep state chosen is dominant compared to all other orbitals at that en-

TABLE I. Relative shift of band-edges in eV as calculated using a deep s state (Deep-state) and aligning the electrostatic potential (Electrostatic).

Method	$Lu_3Ga_5O_{12}$	$Gd_3Al_5O_{12}$
Deep-state	1.9	0.4
Electrostatic	2.1	0.6

ergy making it an ideal candidate for band alignment as this state is insensitive to the local coordination of the atoms and thus should have the same energy regardless of environment. With this deep state identified, band-edges of two systems then can be compared directly by shifting the band structure of one such that the energy of the deep state coincides with the same state in the other structure.

To validate the approach of employing the computationally less intensive deep state approach, we compared the relative shift with the average electrostatic potential for two cases (Al substitution with Ga, and Lu substitution with Gd). Fig. 2(b) shows the supercell used for calculating the average electrostatic potential. The offset between the two systems was calculated using the average electrostatic potentials for $Lu_3Al_5O_{12}$ and $Lu_3Ga_5O_{12}$ and $Lu_3Al_5O_{12}$ and $Gd_3Al_5O_{12}$. Table I shows the good agreement between the two methods for calculating the band offset, providing confidence that the deep s state approach gives physically meaningful values.

III. RESULTS

A. Al substitution

First we consider the extreme case of full Al substitution with larger cations. Using the deep s state of oxygen as the common reference, we calculated the relative position of band-edges of various $Lu_3B_5O_{12}$ compounds, where B=(Al, Ga, In, As, and Sb). Other garnets are less common than Al garnets, with only $Lu_3Ga_5O_{12}$ [38–40] and $Lu_3Sb_5O_{12}$ [41] reported in literature. However, analyzing how other B cations impact the electronic structure may guide future doping and admixing strategies where full substitution may not be required. Figure 3(a) shows the relative position of the conduction band minimum (CBM) and valence band maximum (VBM), along with the lattice parameters, for each of the compounds considered. Figure 3(b) shows the change in band-gap as a function of lattice parameter.

The experimental band-gap of $Lu_3Al_5O_{12}$ is 7.5-8.0 eV [42] which is in reasonably good agreement with the hybrid density functional theory calculated band-gap of 6.9 eV. However, what is important to this study is the relative change of band-gap energy (rather than absolute value), and this is predicted well with PBE. That is, the

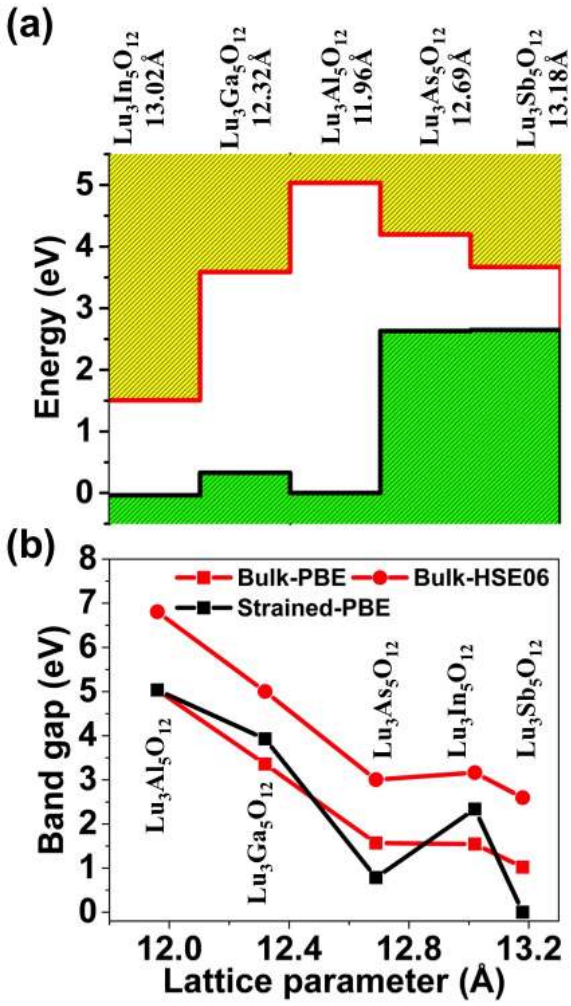

FIG. 3. (a) Conduction and valence band change for $Lu_3B_5O_{12}$ compounds, where B = Al, In, Ga, As and Sb. (b) Change in band-gap as a function of lattice parameter for the different compounds considered. The "bulk" (red) line indicates the band-gap of the compound at its relaxed lattice constant (calculated using PBE and HSE06) while the "strained" (black) line is the band-gap of the compound when placed at the lattice constant of $Lu_3Al_5O_{12}$, to better separate the roles of chemistry and strain on the changes in the band-gap. The band-gap for the strained compound is plotted versus the compound's natural lattice constant, for ease of comparison.

change in band-gap as calculated with both methods is in very good agreement. We had shown this before for ZnX (X= O, S, Se, and Te) compounds under uniaxial strains with d electrons [43, 44]. This work indicates that PBE accurately predicts band-edge shifts even for materials with correlated electrons.

There are several observations that can be made from from Fig. 3. First, $Lu_3Al_5O_{12}$ (LuAG) has the largest band-gap of all compounds considered, and the band-gap decreases with increasing lattice parameter. As has been observed previously, for $Lu_3Ga_5O_{12}$ (LGG) the CBM is

shifted with respect to LuAG, while the VBM is only slightly shifted and this shift in the CBM of LGG is related to the CBM shift observed in Ga-doped LuAG, which leads to the overlap of the cation antisite trap state [29]. A similar, but more pronounced, effect is observed for $Lu_3In_5O_{12}$, where the CBM is further shifted with respect to LuAG and LGG, but the VBM remains near to that of LuAG and LGG. Overall, while the VBM remains essentially constant when substituting Al with In and Ga, large CBM variations are observed. However, substituting Al with either As or Sb leads to significantly larger changes in the VBM while the associated shifts in the CBM are relatively modest, see Figure 3. Thus, upon substitution of Al with As or Sb, the overall decrease in the band-gap is primarily due to increased VBM energy. Although the VBM shifts observed for $Lu_3As_5O_{12}$ and $Lu_3Sb_5O_{12}$ are similar, the larger $Lu_3Sb_5O_{12}$ exhibits a larger CBM shift.

The difference between $Lu_3As_5O_{12}$/$Lu_3Sb_5O_{12}$ (i.e large VBM shift) and $Lu_3In_5O_{12}$/$Lu_3Ga_5O_{12}$ (i.e. large CBM shift) can be understood by closely examining the states that constitute the CBM and VBM. For example, Fig. 4 shows the electronic density of states (DOS) for $Lu_3Al_5O_{12}$, $Lu_3Ga_5O_{12}$, and $Lu_3In_5O_{12}$. The DOS of $Lu_3Al_5O_{12}$ shows that the CBM is comprised of a Lu *d* state and the VBM is dominated by an O *p* state. In $Lu_3Ga_5O_{12}$ and $Lu_3In_5O_{12}$, the CBM shift is driven by Ga and In *s* states hybridizing with the O *p* state, which are, in these two cases, dominant contributors to the CBM. Figure 5 shows the DOS for $Lu_3Al_5O_{12}$, $Lu_3As_5O_{12}$, and $Lu_3Sb_5O_{12}$. In $Lu_3As_5O_{12}$ and $Lu_3Sb_5O_{12}$ the VBM shift is driven by As and Sb *s* states hybridizing with the O *p* state which are now dominant contributors to the VBM. This situation is similar to a shift of VBM in TiO_2 that has been observed when S is substituted with O due to the strong hybridization of S and O p states [45]. In addition to the prominent difference in hybridization of states in the two cases, Bader charge analysis shows that As and Sb bonds are more covalent compared to Ga and In bonds [46, 47]. Thus, and as expected, more pronounced covalent bonding dopants such as As and Sb push the VBM higher in energy while ionic (electronegative) bonding dopants such as Ga and In shift the CBM down in energy to reduce the overall band-gap.

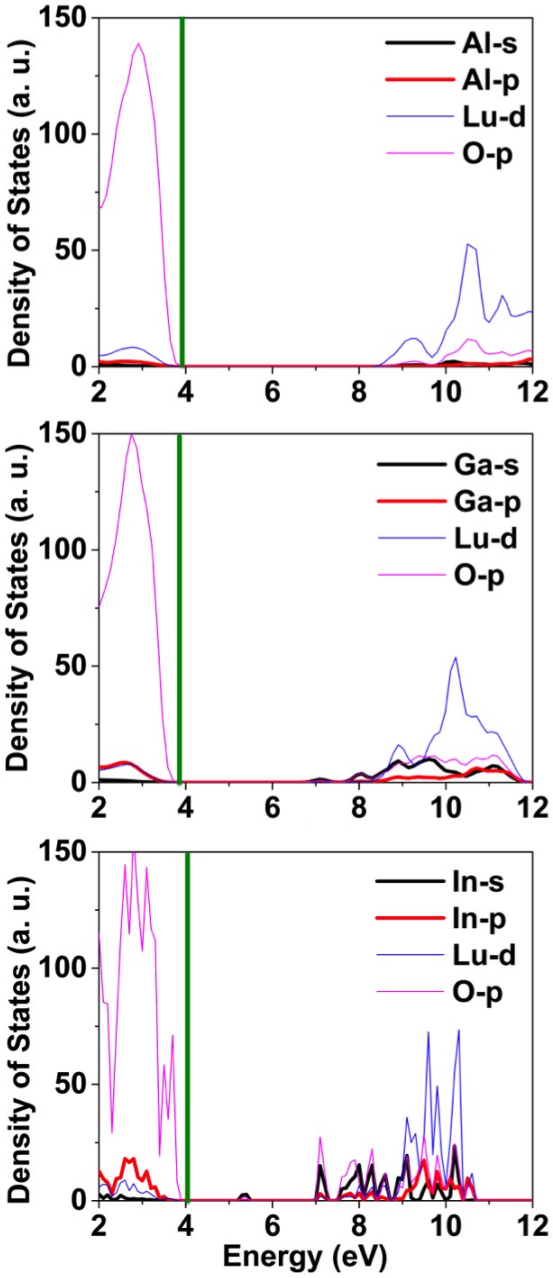

FIG. 4. Density of states arising from Al, Ga, In *s* and *p* states, Lu *d* states and O *p* states for garnets with B=Al, Ga, and In. The green vertical line corresponds to the Fermi level (highest occupied state), obtained by the alignment of the deep oxygen s state.

B. Electronic structure variation due to Lu substitution

Now we move to extreme case of full Lu substitution with Gd, Dy and Er to assess the effect of admixing on the RE site on the band-gap and band-edges of LuAG. The relative position of the band-edges of $RE_3Al_5O_{12}$ (where RE = Lu, Gd, Dy, and Er) is shown in Fig. 6(a). Fig. 6(b) shows the change in the band-gap as a function of lattice parameter. Substituting Lu with Gd, Dy or Er results in relatively small shifts in the band-gap, which is commensurate with negligible variations in lattice parameter. In all cases the VBM and the CBM shift in the same direction, resulting in an overall band-gap that is relatively constant. It is also interesting to note that Lu, Gd, Dy, and Er *5d* states dominate the bottom of the conduction band.

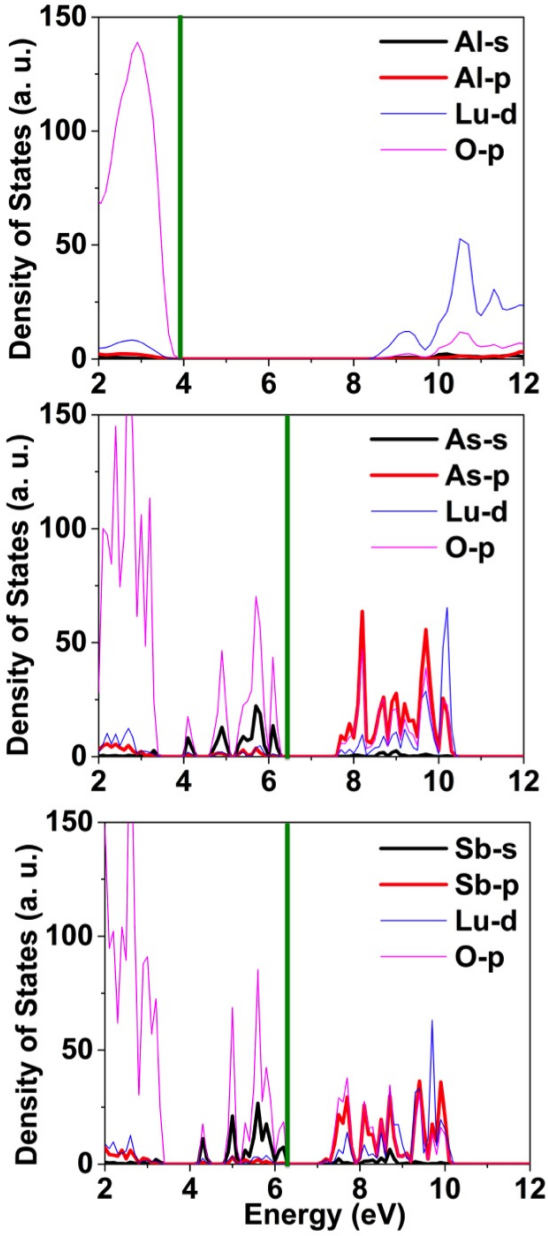

FIG. 5. Density of states arising from Al, As, Sb s and p states, Lu d states and O p states for garnets with B=Al, As, and Sb. The green vertical line corresponds to the Fermi level (highest occupied state), obtained by the alignment of the deep oxygen s state.

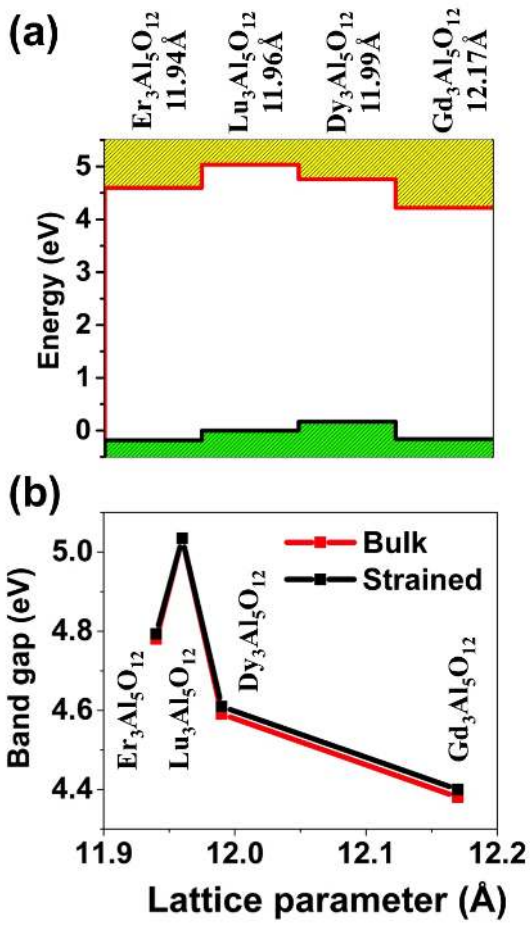

FIG. 6. (a) Conduction and valence band changes for $RE_3Al_5O_{12}$ compounds, where RE = Lu, Gd, Dy and Er. (b) Change in band-gap as a function of lattice parameter for the different compounds considered. The "bulk" (red) line indicates the band-gap of the compound at its relaxed lattice constant while the "strained" (black) line is the band-gap of the compound when placed at the lattice constant of $Lu_3Al_5O_{12}$. The band-gap for the strained compound is plotted versus the compound's natural lattice constant, for ease of comparison.

C. Effect of admixing concentration

Finally, we have assessed the role of admixed species concentration on band structure. That is, the above results only consider full substitution of Lu or Al cations in $Lu_3Al_5O_{12}$ rather than a partial replacement of Al or Lu, which is a more realistic scenario. Given that Gd and Ga are present in some of the multicomponent garnet compounds of interest for scintillating applications, we have systematically assessed how variations in their concentration modify the band-gap and band-edge position.

Figure 7(a) shows the variation in the band-gap, (b) CBM and (c) VBM as a function of Ga (x) and Gd (y) concentration in $(Lu_{1-x}Gd_x)_3(Al_{1-y}Ga_y)_5O_{12}$. The garnet structure contains one crystallographically unique Lu site but two crystallographically unique Al sites, of which 40% are octahedrally coordinated and 60% are tetrahedrally coordinated. We used the special quasirandom structure (SQS)[48] approach to generate representative structures that mimic randomly substituted Ga and Gd amongst all of the sites. In generating the SQSs, we considered the tetrahedral and octahedral sublattices as distinct and constructed SQSs in which the cations were distributed independently on these two sublattices. These SQSs were then combined to achieve the various levels of

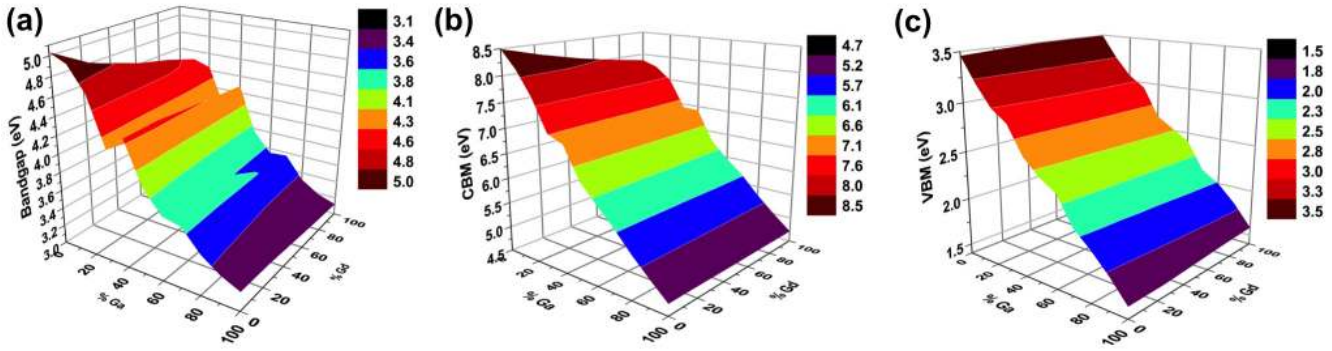

FIG. 7. Variation of band-gap (eV), CBM (eV), and VBM (eV) as a function of B (B= Ga, In, As and Sb) substituting for Al substituting for Lu in $(Lu_3(Al_{1-x}B_x)_5O_{12}$.

substitutional species. This lead to situations in which all of the substitutional species were on tetrahedral sites for one composition (e.g. 30%) and all on octahedral sites for the next composition (40%), leading to discontinuities in the properties between those compositions. However, the change in band-gap depends more significantly on the total Ga content and less on the actual distribution between tetrahedral and octahedral sites.

It can be seen that the variation in band-gap with Gd concentration is quite linear. The only deviation from linearity is observed when the position of the Ga switches from the octahedral to the tetrahedral site, as discussed above. Ga present on tetrahedral sites leads to a larger reduction in band-gap and a larger CBM shift than when Ga is present on octahedral sites. Hence there is abrupt shift from 30% to 40%, when Ga substitution transitioned from all tetrahedral (at 30%) to all octahedral (at 40%) sites. In a truly random distribution of Ga, this abrupt shift would not occur and the dependence on the band-gap and CBM shift on the Ga concentration would be linear throughout the composition range. Furthermore, and as discussed above for the cases of full substitution, the change in band-gap is much more sensitive to changes in the B cation than the A cation. Over most of the compositional range, the band-gap is relatively insensitive to the Gd concentration, except for when the Ga content is very small. All of the change in the band-gap in this compositional range is due to Ga-induced changes in the CBM.

The calculations of LuAG admixed with Ga suggested a linear relationship between band-edge shifts and Ga concentration. To verify the generality of linear band-gap variation as a function of Al substituent concentration in $Lu_3Al_5O_{12}$, we also calculated band-gap variations for In, As, and Sb substituting for Al as a function of admixed concentration, see Fig. 8. At small concentrations, In, As, and Sb have a more significant effect on the band-gap variation compared to Ga. An implication of this result is that doping with a smaller concentration of In compared to Ga will have the same effect on the CBM. Also, the band-gap shift resulting from As and Sb doping is markedly different from Ga. Specifically, there are

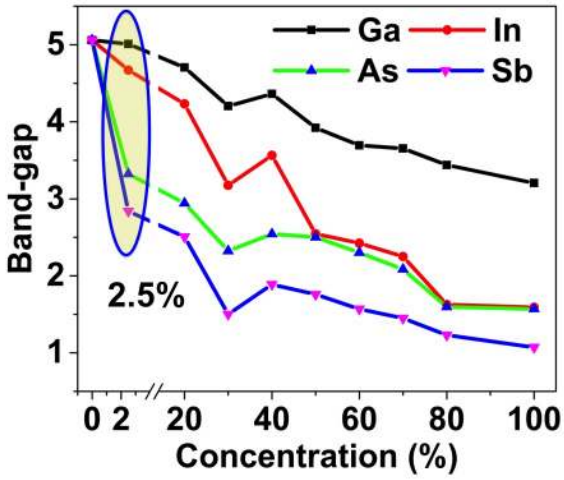

FIG. 8. Variation of band-gap (eV) as a function of B (B= Ga, In, As, and Sb) concentration, substituting for Al in $Lu_3(Al_{1-x}B_x)_5O_{12}$. The smallest possible concentration in our simulation cells, 2.5%, is highlighted by the circle.

two regimes, where the biggest shift in band-gap occurs at relatively low concentrations and above 40% As or Sb, the band-gap shift is again linear and similar to Ga. That is, after an initial large shift in the band-gaps induced by In or As, the subsequent changes are similar to those induced by Ga. The sharp initial drop in the band-gap due to doping with either As or Sb can be interpreted as follows. With a small amount of dopant, a deep dopant level is created that forms the new valence band-edge. With increasing dopant concentration, the new valence band widens and consequently further reduces the band gap, but only modestly compared to the initial drop. Further, the results in Fig. 8 suggest that band-gap changes induced by ionic species such as In and Ga are relatively linear while those produced by more covalent materials exhibit a less linear but still monotonic dependence on admixed ion concentration.

IV. DISCUSSION

Our results suggest that both strain and chemistry play important roles in determining the band-gap and relative position of band-edges in $A_3B_5O_{12}$ garnets. Cations with larger radii tend to produce smaller band-gaps. This is accompanied by an increase in the lattice parameter. This suggests that the cation radius can be used as an initial screening parameter in the search for candidate dopants to modify the band-gap. However, while we have considered extreme limits of full substitution, some of these hypothetical compounds may not be realizable experimentally. This may explain the need to co-dope $Lu_3Al_5O_{12}$ with both Ga and Gd. Gd, having a larger radius than Lu, would help maintain the A/B radius ratio in $A_3B_5O_{12}$ garnets, stabilizing the compound. Further, also a consequence of the larger size, Gd would suppress excess antisite formation between the A and B sites as it would increase the average disparity in cation size between the two sites.

It might also be advantageous to dope or admix with smaller amounts of larger cations. For example, the band-gap change for In-substituted LuAG is much larger than for Ga-substituted LuAG. One might be able to achieve the same shifts in the CBM exhibited for full substitution of Ga by relatively modest amounts of In substitution. This would provide for more opportunities for admixing strategies, as discussed below.

To better isolate the roles of strain and chemistry, we calculated the band-gap of all of the compounds considered when they are strained to the lattice constant of $Lu_3Al_5O_{12}$. These results are shown in Fig. 3(b) and 6(b) with the line labeled "strained". For both Al and Lu substitution, the band-gap for the compounds at their natural lattice constant and when strained to the $Lu_3Al_5O_{12}$ lattice constant show very similar behavior. This indicates that the changes in the band-edges are not simply a consequence of strain induced by changing the radii of the cations, but rather is an effect inherent in the chemistry of the cations. Thus, while the cation radius seems to correlate with the changes in band-gap, it is not a direct cause of those changes.

Our results suggest admixing strategies to finely tune the band-edges of complex oxide compounds for applications such as scintillators. One can imagine admixing LuAG with both Ga and As, the first to lower the CBM and remove electron traps and the second to raise the VBM and eliminated hole traps. An implication of the non linear variation of band-edges is, very small amount of In, As, and Sb would have much larger effect on band-edges . Of course, the stability of such chemically complex garnets must be examined, but by choosing the appropriate dopant species and concentrations, the band-edges, in principle, can be tuned to very precise values. In fact, the results in Fig. 3 suggest that if one were to co-dope with In and either As or Sb, the band-gap might be eliminated altogether. If such a compound is not thermodynamically stable, there might be other dopants that can achieve the same effect. In addition, in multicomponent garnets a positive effect on light yield is also expected due to local chemical composition fluctuation and related band-edges fluctuation which may limit the out-of-track migration of charge carriers thus supporting their immediate radiative recombination at emission centers [49].

Ce^{3+} is a typical dopant used as a center for photoluminescence. The upward shift of the VBM with admixing by As and Sb will reduce the energy gap between the VBM and the Ce^{3+} ground state, which might facilitate the hole transfer from the valence band towards the Ce^{3+} center in multicomponent garnet hosts. In YAG, LuAG and GGAG this energy gap has been estimated to be about 3.6 eV [15]. Such a large energy gap can indeed lower the probability of fast hole transfer towards Ce^{3+}. An optimum gap value in this case is usually considered within 0.5-1 eV [50]. Thus, with the right concentrations of As or Sb, this VBM-Ce gap can be reduced to optimal values.

V. CONCLUSIONS

Admixing $RE_3Al_5O_{12}$ garnet compounds with Ga and Gd has led to pronounced improvements in scintillator performance, in part due to shifts in the conduction band such that the energy level of shallow defects is no longer in the forbidden gap. In this work we screen for additional admixing species using first-principles DFT, focusing on the variation of band-edges in order to potentially "band-edge engineer" next-generation garnet scintillators. We have shown that certain dopants can influence the VBM or the CBM or both, which opens the door for further admixing strategies to optimize scintillator compounds. We show that substituting Al with Ga, In, As, and Sb in LuAG changes the band-gap, with ionic elements (Ga and In) tend to decrease the band-gap by lowering the CBM, and, on the other hand, covalent elements (Sb and As) tending to decrease the band-gap by pushing the VBM higher in energy. In contrast, substituting Lu with Gd, Dy or Er changes neither the band-gap nor the band-edges to any significant degree. This study opens the possibility of tuning band-gaps and band-edges by admixing not only garnets but other complex oxides as well. The ability to control band-gap and band-edges independently is a powerful tool to optimize the performance of various materials for technological applications including not only scintillation, but also solar cells, light emitting diodes, and field effect transistors that require proper alignment of band-edges across heterostructures.

ACKNOWLEDGMENTS

BPU was supported by the U.S. Department of Energy, Office of Science, Basic Energy Sciences, Materials Sci-

ences and Engineering Division. MN acknowledges partial support of Czech National Science foundation grant no. P204/12/0805. CRS and SKY gratefully acknowledge support of the Nonproliferation Research and Development program within the U.S. National Nuclear Security Administration. Los Alamos National Laboratory, an affirmative action equal opportunity employer, is operated by Los Alamos National Security, LLC, for the National Nuclear Security Administration of the U.S. DOE under contract DE-AC52-06NA25396.

[1] J. Geusic, H. Marcos, and L. Vanuitert, Laser oscillations in Nd-doped yttrium aluminum, yttrium gallium and gadolinium garnets Appl. Phys. Lett. **4**, 182 (1964).

[2] G. Blasse and A. Bril, A new phosphor for flying-spot cathode-ray tubes for color television: yellow-emitting $Y_3Al_5O_{12}$-Ce^{3+} Applied Physics Letters **11**, 53 (1967).

[3] M. Weber, Nonradiative decay from 5d states of rare earths in crystals, Solid State Commun. **12**, 741 (1973).

[4] M. Moszynski, T. Ludziejewski, D. Wolski, W. Klamra, and L. Norlin, Properties of the YAG: Ce scintillator Nucl. Inst. Meth. A **345**, 461 (1994).

[5] M. Weber, Scintillation: mechanisms and new crystals, Nucl. Inst. Meth. A **527**, 9 (2004).

[6] M. Nikl, E. Mihokova, J. Pejchal, A. Vedda, M. Fasoli, I. Fontana, V. Laguta, V. Babin, K. Nejezchleb, A. Yoshikawa, Scintillator materials-achievements, opportunities, and puzzles, et al., Nuclear Science, IEEE Transactions on **55**, 1035 (2008).

[7] T. Kanai, M. Satoh, and I. Miura, Characteristics of a nonstoichiometric Gd^{3+} δ (Al, Ga)$_5$-δO_{12}: Ce garnet scintillator, Journal of the American Ceramic Society **91**, 456 (2008).

[8] N. Cherepy, J. Kuntz, Z. Seeley, S. Fisher, O. Drury, B. Sturm, T. Hurst, R. Sanner, J. Roberts, and S. Payne, SPIE Optical Engineering + Applications (International Society for Optics and Photonics, 2010),

[9] K. Kamada, T. Yanagida, J. Pejchal, M. Nikl, T. Endo, K. Tsutumi, Y. Fujimoto, A. Fukabori, and A. Yoshikawa, Scintillator-oriented combinatorial search in Ce-doped (Y, Gd)$_3$(Ga, Al)$_5$O$_1$2 multicomponent garnet compounds, Journal of Physics D: Applied Physics **44**, 505104 (2011).

[10] K. Kamada, T. Endo, K. Tsutumi, T. Yanagida, Y. Fujimoto, A. Fukabori, A. Yoshikawa, J. Pejchal, and M. Nikl, Composition engineering in cerium-doped (Lu,Gd)$_3$(Ga, Al)$_5O_{12}$ single-crystal scintillators, Crystal Growth & Design **11**, 4484 (2011).

[11] M. Nikl, A. Yoshikawa, K. Kamada, K. Nejezchleb, C. R. Stanek, J. Mares, and K. Blazek, Development of LuAG-based scintillator crystals-a review, Progress in Crystal Growth and Characterization of Materials **59**, 47 (2013).

[12] M. Tyagi, F. Meng, M. Koschan, S. B. Donnald, H. Rothfuss, and C. L. Melcher, Effect of codoping on scintillation and optical properties of a Ce-doped $Gd_3Ga_3Al_2O_{12}$ scintillator, Journal of Physics D: Applied Physics **46**, 475302 (2013).

[13] J. M. Ogiegło, A. Katelnikovas, A. Zych, T. Jstel, A. Meijerink, and C. R. Ronda, Luminescence and luminescence quenching in Gd_3(Ga, Al)$_5O_{12}$ scintillators doped with Ce^{3+}, The Journal of Physical Chemistry A **117**, 2479 (2013).

[14] W. Drozdowski, K. Brylew, M. Witkowski, A. Wojtowicz, P. Solarz, K. Kamada, and A. Yoshikawa, Studies of light yield as a function of temperature and low temperature thermoluminescence of $Gd_3Al_2Ga_3O_{12}$: Ce scintillator crystals, Optical Materials **36**, 1665 (2014).

[15] Y. Wu, F. Meng, Q. Li, M. Koschan, and C. L. Melcher, Role of Ce^{4+} in the Scintillation Mechanism of Co-doped $Gd_3Ga_3Al_2O_{12}$: Ce, Physical Review Applied **2**, 044009 (2014).

[16] P. Sibczynski, J. Iwanowska-Hanke, M. Moszynski, L. Swiderski, M. Szawlowski, M. Grodzicka, T. Szczesniak, K. Kamada, and A. Yoshikawa, Characterization of GAGG: Ce scintillators with various Al-to-Ga ratio, Nuclear Instruments and Methods in Physics Research Section A: Accelerators, Spectrometers, Detectors and Associated Equipment **772**, 112 (2015).

[17] M. Nikl, A. Yoshikawa, K. Kamada, K. Nejezchleb, C. R. Stanek, J. Mares, and K. Blazek, Development of LuAG-based scintillator crystals - A review, Prog. Cryst. Growth Char. Mater. **59**, 47 (2013).

[18] V. Lupei, A. Lupei, C. Tiseanu, S. Georgescu, C. Stoicescu, and P. Nanau, High-resolution optical spectroscopy of YAG: Nd: a test for structural and distribution models, Phys. Rev. B **51**, 8 (1995).

[19] M. Nikl, E. Mihokova, J. Pejchal, A. Vedda, Y. Zorenko, and K. Nejezchleb, The antisite LuAl defect-related trap in $Lu_3Al_5O_{12}$: Ce single crystal, phys. stat. sol. b **242**, R119 (2005).

[20] H. Donnerberg and C. Catlow, Atomistic computer simulations of yttrium iron garnet (YIG) as an approach to materials defect chemistry. I. Intrinsic defects, J. Phys.: Condens. Matt. **5**, 2947 (1993).

[21] M. M. Kuklja, Defects in yttrium aluminium perovskite and garnet crystals: atomistic study, J. Phys.: Condens. Matt. **12**, 2953 (2000).

[22] C. Milanese, V. Buscaglia, F. Maglia, and U. Anselmi-Tamburini, Disorder and nonstoichiometry in synthetic garnets $A_3B_5O_{12}$ (A= Y, Lu-La, B= Al, Fe, Ga). a simulation study, Chem. Mater. **16**, 1232 (2004).

[23] C. R. Stanek, K. McClellan, M. Levy, C. Milanese, and R. Grimes, The effect of intrinsic defects on $RE_3Al_5O_{12}$ garnet scintillator performance, Nucl. Instrum. Methods A **579**, 27 (2007).

[24] M. Nikl, The antisite LuAl defect-related trap in $Lu_3Al_5O_{12}$: Ce single crystal, phys. stat. sol. (a) **202**, 201 (2005).

[25] M. Nikl, J. Pejchal, E. Mihokova, J. Mares, H. Ogino, A. Yoshikawa, T. Fukuda, A. Vedda, and C. D'Ambrosio, Antisite defect-free $Lu_3(Ga_xAl_{1-x})_5O_{12}$: Pr scintillator Appl. Phys. Lett. **88**, 141916 (2006).

[26] R. Shannon, Revised Effective Ionic Radii and Systematic Studies of Interatomic Distances in Halides and Chalcogenides, Acta Cryst. A **32**, 751 (1976).

[27] G. Shirinyan, K. Ovanesyan, A. Eganyan, A. Petrosyan, C. Pedrini, C. Dujardin, I. Kamenskikh, and N. Guerrassimova, X-ray and optical studies of ytterbium-doped

gallium garnets, Nucl. Inst. Meth. A **537**, 134 (2005).
[28] C. R. Stanek, C. Jiang, S. K. Yadav, K. McClellan, B. P. Uberuaga, D .A. Andersson, and M. Nikl, The effect of Ga-doping on the defect chemistry of $RE_3Al_5O_{12}$ garnets, Phys. Stat. Sol. B **250**, 244 (2013).
[29] M. Fasoli, A. Vedda, M. Nikl, C. Jiang, B. P. Uberuaga, D. A. Andersson, K. McClellan, and C. R. Stanek, Band-gap engineering for removing shallow traps in rare-earth $Lu_3Al_5O_{12}$ garnet scintillators using Ga^{3+} doping, Phys. Rev. B **84**, 081102(R) (2011).
[30] G. Kresse and J. Furthmüller, Efficient iterative schemes for ab initio total-energy calculations using a plane-wave basis set, Physical Review B **54**, 11169 (1996).
[31] J. P. Perdew, K. Burke, and M. Ernzerhof, Generalized gradient approximation made simple, Physical review letters **77**, 3865 (1996).
[32] P. E. Blöchl, Projector augmented-wave method, Physical Review B **50**, 17953 (1994).
[33] A. V. Krukau, O. A. Vydrov, A. F. Izmaylov, and G. E. Scuseria, Influence of the exchange screening parameter on the performance of screened hybrid functionals., The Journal of chemical physics **125**, 224106 (2006).
[34] S.-H. Wei and A. Zunger, Band offsets and optical bowings of chalcopyrites and Zn-based II-VI alloys, Journal of Applied Physics **78**, 3846 (1995).
[35] P. G. Moses and C. G. Van de Walle, Band bowing and band alignment in InGaN alloys, Applied Physics Letters **96**, 021908 (2010).
[36] C. G. Van de Walle and R. M. Theoretical calculations of heterojunction discontinuities in the Si/Ge system, Martin, Physical Review B **34**, 5621 (1986).
[37] A. Franciosi and C. G. Van de Walle, Heterojunction band offset engineering, Surface Science Reports **25**, 1 (1996).
[38] V. Venkatramu, M. Giarola, G. Mariotto, S. Enzo, S. Polizzi, C. Jayasankar, F. Piccinelli, M. Bettinelli, and A. Speghini, Nanocrystalline lanthanide-doped $Lu_3Ga_5O_{12}$ garnets: interesting materials for light-emitting devices, Nanotechnology **21**, 175703 (2010).
[39] X. Xu, J. Chen, S. Deng, N. Xu, and J. Lin, Cathodoluminescent properties of nanocrystalline $Lu_3Ga_5O_{12}$: Tb^{3+} phosphor for field emission display application, Journal of Vacuum Science & Technology B **28**, 490 (2010).
[40] V. Mahalingam, F. Mangiarini, F. Vetrone, V. Venkatramu, M. Bettinelli, A. Speghini, and J. A. Capobianco, Bright white upconversion emission from $Tm^{3+}/Yb^{3+}/Er^{3+}$-doped $Lu_3Ga_5O_{12}$ nanocrystals, The Journal of Physical Chemistry C **112**, 17745 (2008).
[41] A. Raevsky, A. Gukalova, and G. Semin, Nuclear quadrupole resonance of antimony in $Ln_3Sb_5O_{12}$ crystals, Zeitschrift für Naturforschung. A, A Journal of physical sciences **49**, 687 (1994).
[42] Y. Zorenko, V. Gorbenko, I. Konstankevych, A. Voloshinovskii, G. Stryganyuk, V. Mikhailin, V. Kolobanov, and D. Spassky, Single-crystalline films of Ce-doped YAG and LuAG phosphors: advantages over bulk crystals analogues, Journal of Luminescence **114**, 85 (2005).
[43] S. K. Yadav and R. Ramprasad, Applied Physics Letters **100**, 241903 (2012).
[44] S. K. Yadav, V. Sharma, and R. Ramprasad, Controlling electronic structure through epitaxial strain in ZnSe/ZnTe nano-heterostructures, Journal of Applied Physics **118**, 015701 (2015).
[45] K. Yang, Y. Dai, and B. Huang, The Journal of Physical Chemistry C **111**, 18985 (2007).
[46] R. F. Bader, *Atoms in molecules* (Wiley Online Library, 1990).
[47] W. Tang, E. Sanville, and G. Henkelman, A grid-based Bader analysis algorithm without lattice bias, Journal of Physics: Condensed Matter **21**, 084204 (2009).
[48] A. Zunger, S.-H. Wei, L. Ferreira, and J. E. Bernard, Special quasirandom structures, Physical Review Letters **65**, 353 (1990).
[49] A. V. Gektin, A. N. Belsky, and A. N. Vasil'ev, Scintillation efficiency improvement by mixed crystal use, Nuclear Science, IEEE Transactions on **61**, 262 (2014).
[50] P. Dorenbos, Fundamental Limitations in the Performance of Ce^{3+}, Pr^{3+} and - Eu^{2+} Activated Scintillators, Nuclear Science, IEEE Transactions on **57**, 1162 (2010).